Myocardial Bridging of the Left Anterior Descending Coronary Artery: Depiction Rate and Morphologic Features by Dual-Source CT Coronary Angiography

Jin Ho Hwang, MD[1]
Sung Min Ko, MD[1]
Hong Gee Roh, MD[1]
Meong Gun Song, MD[2]
Je Kyoun Shin, MD[2]
Hyun Kun Chee, MD[2]
Joon Suk Kim, MD[2]

Objective: To evaluate the depiction rate and morphologic features of myocardial bridging (MB) of the left anterior descending coronary artery (LAD) using dual-source CT (DSCT).

Materials and Methods: CT scans from a total of 1,353 patients who underwent DSCT were reviewed retrospectively for LAD-MB. Seventy-eight patients were excluded due to poor image quality or poor enhancement of the coronary artery. The length and depth of the MB were analyzed and classified as superficial or deep with respect to the depth ($\leq$ 1 or > 1 mm) of the LAD tunneled segment. Superficial MB was subdivided into complete or incomplete types according to full or partial encasement of the myocardium.

Results: Of the 1,275 patients included in this study, 557 cases of MB were found from 536 patients (42%). Superficial MB was observed in 368 of 557 (66%) cases, and deep MB was seen in 189 of 557 (34%) cases. Superficial MB showed 2 types: complete (128 of 368, 35%) and incomplete (240 of 368, 65%). The mean length of a tunneled segment for superficial MB was 16.4 $\pm$ 8.6 mm. The mean length and depth of a tunneled segment for deep MB were 27.6 $\pm$ 12.8 mm and 3.0 $\pm$ 1.4 mm, respectively. The incidence of atherosclerotic plaques in a 2-cm-long segment proximal to MB was 16%.

Conclusion: The depiction rate of LAD-MB using DSCT in a large series of patients was 42%, with two-thirds of MB segments being the superficial type.

Index terms:
Myocardial bridging
Computed tomography (CT)
Dual-source CT
CT coronary angiography
Conventional angiography
Coronary arteries

DOI:10.3348/kjr.2010.11.5.514

Korean J Radiol 2010;11:514-521
Received April 2, 2010; accepted after revision May 26, 2010.

Departments of [1]Radiology and [2]Thoracic Surgery, Konkuk University Hospital, Konkuk University School of Medicine, Seoul 143-729, Korea

This work was supported by the Konkuk University Medical Center Research Grant in 2008.

Corresponding author:
Sung Min Ko, MD, Department of Radiology, Konkuk University Hospital, Konkuk University School of Medicine, 4-12 Hwayang-dong, Gwangjin-gu, Seoul 143-729, Korea.
Tel. (822) 2030-5578
Fax. (822) 2030-5549
e-mail: ksm9723@yahoo.co.kr

Myocardial bridging (MB) is a congenital condition in which a segment of a major epicardial coronary artery proceeds intramurally through the myocardium beneath the muscle bridge. Although MB is thought to be a normal variant and is clinically silent in most cases, it has sometimes been associated with myocardial ischemia, myocardial infarction, arrhythmia, and sudden death (1–6). The left anterior descending coronary artery (LAD) is the most commonly involved site. Even though systolic compression of the tunneled segment alone cannot sufficiently explain the clinical significance of MB, the length and depth of MB of the LAD may be clinically important. Traditionally, conventional coronary angiography (CCA) has been considered to be the gold standard for the detection of systolic compression of the tunneled segment. However, the depiction rate of MB with CCA is only 0.5–4.5% of the general population when compared to the incidence of MB in autopsy studies (15–85%) (1–6); this difference suggests that CCA is not sensitive enough to detect MB, particularly superficial MB.

The use of multi-detector computed tomography (MDCT) coronary angiography (CA) has been accepted as a reliable and sensitive imaging modality for the depiction

of MB (7–9). The depiction rate of MB reported in a CT coronary angiography (CTCA) series has ranged from 4% to 58% (10–27), depending on the types of MDCT scanners and inclusion or exclusion of superficial MB. The recently used dual-source CT (DSCT), in which two X-ray tubes and two corresponding detectors are used at the same time, allows for a much improved temporal resolution of 83 msec. The improved temporal resolution reduces cardiac motion artifact and therefore enables clear visualization of the vessel lumen during most of the cardiac cycle. Lu et al. (19) reported that DSCT detected more cases of MB than CCA (30% vs. 6%) in 53 patients. However, to the best of our knowledge, there has been no report about the depiction rate and the morphologic features of MB of the LAD using DSCT in a large patient population. Thus, the aim of our study was to evaluate the depiction rate and the morphologic features of MB of the LAD using DSCT.

MATERIALS AND METHODS

Study Population

The study was approved by our hospital's Institutional Review Board. Written informed consent was not required because of the retrospective nature of the investigation. Between June and December of 2008, 1,353 consecutive patients (613 males, 740 females) who underwent CTCA were reviewed for the evaluation of MB. The indications for CTCA were as follows: typical chest pain (n = 152), atypical chest pain (n = 348), non-anginal chest pain (n = 175), known coronary artery disease (CAD) (n = 71), valvular heart disease (n = 189), presence of risk factors for CAD (n = 283), cardiomyopathy (n = 12), congenital heart disease (n = 27), and arrhythmia (n = 96).

Dual-Source CT Coronary Angiography

Prior to the examination, each patient's the heart rate (HR) was measured. Patients with a pre-scan HR > 65 beats per minute (bpm) were given 50–100 mg metoprolol orally, one hour before the scan. All patients received 0.6 mg nitroglycerin sublingually, one minute before the examination, to dilate the coronary arteries. All CT examinations were performed using a DSCT scanner (Somatom Definition, Siemens Medical Solutions, Forchheim, Germany). DSCT was performed from 1 cm below the level of the tracheal bifurcation to the diaphragm in the craniocaudal direction using the following scanning parameters: collimation of 32 × 0.6 mm, slice acquisition of 64 × 0.6 mm using the z-flying focal spot technique, a gantry rotation time of 330 ms, a pitch of 0.20–0.43 (adapted to HR), tube voltage of 100–120 kV (depending on age and body mass index), and a maximum tube current of 320 mAs per rotation.

Contrast agent application was controlled by a bolus tracking technique. A region of interest was placed into the aortic root, and image acquisition began 7 seconds after the signal density level reached the predefined threshold of 120 Hounsfield units (HU). For all CT examinations, a dual-head power injector (Stellant D; Medrad, Indianola, PA) was used to administer a three-phase bolus at a rate of 4.5 mL/s. First, 70–80 mL of iopromide (Ultravist 370®; Bayer Healthcare, Berlin, Germany) was administered. Next, 45 mL of a 70%-to-30% blend of contrast media and saline was administered followed by 45 mL of saline.

Electrocardiography (ECG)-based tube current modulation was implemented with the Mindose manual, except for patients with mean HRs more than 80 bpm, valvular heart disease, or arrhythmia. The full dose window of 35–85% of the cardiac cycle was used in patients with 65 ≤ HR ≤ 79 bpm, whereas 60–80% of the full dose was used in patients with HR < 65 bpm. A retrospective gating technique was used to synchronize data reconstruction with the ECG signal. A mono-segment reconstruction algorithm that uses the data from a quarter rotation from both detectors was used for image reconstruction.

In each patient, images were previewed automatically, and the optimal phase was selected for post-processing. Whenever necessary, additional images were reconstructed in 5% steps of the R-R interval within the full tube current window. For CTCA images reconstructed from the contrast-enhanced DSCT scan with a slice thickness of 0.75 mm, the reconstruction increment was set at 0.4 mm using a medium-soft tissue convolution kernel (B26f). The

Table 1. Patient Data

	All Patients n (%)	MB Patients n (%)
Patients	1,275	536 (42%)
Mean age, years	59.7	58.6
Male gender	578 (45%)	226 (42%)
Indication for CTCA		
Typical chest pain	152 (11%)	69 (13%)
Atypical chest pain	348 (26%)	150 (28%)
Non-anginal chest pain	175 (13%)	67 (13%)
Known CAD	71 (5%)	28 (5%)
Valvular heart disease	189 (14%)	76 (14%)
Presence of risk factors	283 (21%)	80 (15%)
Cardiomyopathy	12 (1%)	7 (1%)
Congenital heart disease	27 (2%)	11 (2%)
Arrhythmia	96 (7%)	48 (9%)

Note.— Values are percentages. CAD = coronary artery disease, CTCA = computed tomography coronary angiography, MB = myocardial bridging

reconstructed field-of-view was adjusted to exactly encompass the heart (image matrix 512×512 pixels), based on individual anatomy. All reconstructed images were transferred to a workstation (Vitrea 2, version 4; Vital Images, MN), where coronary artery segments of the three main coronary arteries and their major side branches with a luminal diameter of 1.5 mm or larger were classified according to the 15-segment American Heart Association model (15), which we modified by adding segment 16 for a ramus intermedius when present.

Data Analysis

All CT images were analyzed by consensus of two radiologists who were blinded to the CCA findings. The image quality of the LAD was assessed semi-quantitatively with a previously described four-point ranking scale (28) (4, excellent image quality; 3, good image quality; 2, fair image quality; 1, poor image quality). Excellent image quality indicated a clear delineation of the coronary artery without motion artifact. Good image quality was classified as having minor motion artifact and mild blurring of vessel margins. Fair image quality was defined as having moderate motion artifacts and moderately blurred vessel without structure discontinuity. Poor image quality was classified as having severe motion artifact and severely blurred vessel with structure doubling or discontinuity. Image evaluation was performed on the workstation.

Myocardial bridging was diagnosed and evaluated when part of the LAD was located in the interventricular gorge and completely or incompletely surrounded by the left ventricular myocardium. For each tunneled segment, the following parameters were recorded: the location of the

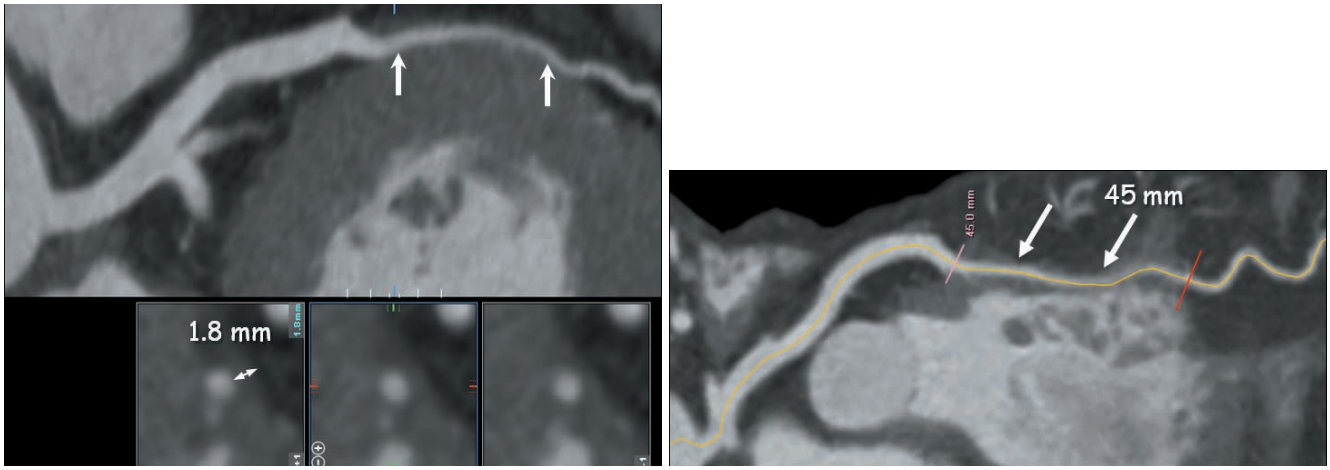

A B

Fig. 1. Depth (**A**) and length (**B**) of tunneled segment (arrows) of left anterior descending coronary artery were analyzed on curved multiplanar reformation images using electronic caliper.

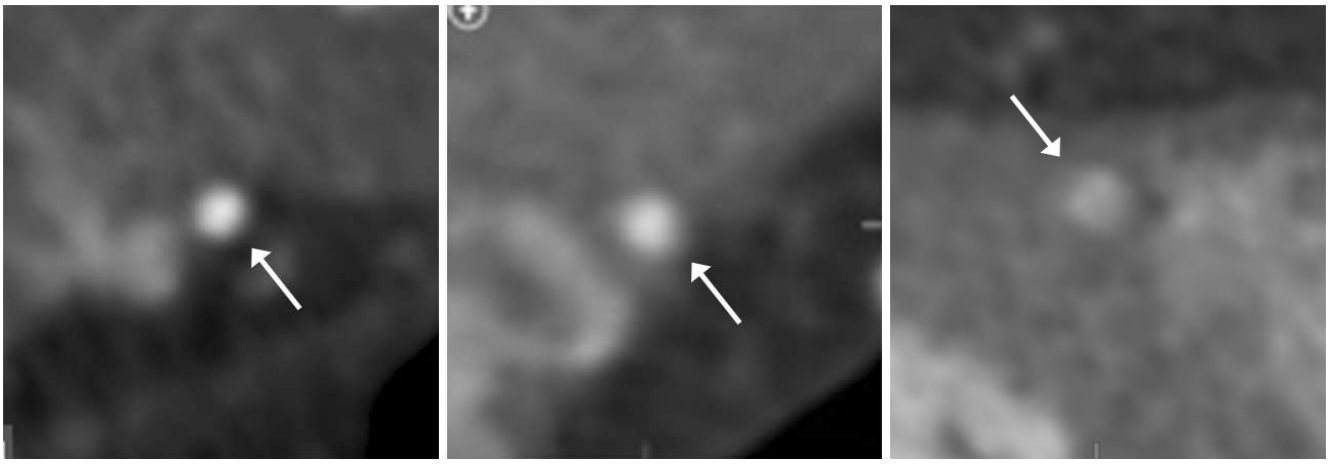

A B C

Fig. 2. Myocardial bridging was classified as superficial (**A, B**) or deep (**C**) according to depth of tunneled segment (arrows) of left anterior descending coronary artery. Superficial type was subdivided into incomplete (**A**) and complete (**B**) types according to extent of vessel encasement by myocardium.

LAD (proximal, middle, and distal), the length and depth of the tunneled segment, and the presence of atherosclerosis in the tunneled segment and in a 2-cm-long segment proximal to the entry of the tunneled segment. The depth and length of the tunneled segment of the LAD were analyzed using dedicated vessel analysis software, particularly measured using an electronic caliper (Fig. 1). The length of the tunneled segment was measured as the length of the myocardial bridge covering the distance between the entrance and the exit of the tunneled segment. The depth of the tunneled segment was measured as the widest part between the surface of the myocardial bridge and the tunneled segment.

The tunneled segments of the LAD were divided as being superficial or deep based on the depth of the tunneled segment (≤ 1 or > 1 mm) (12) (Fig. 2). We also subdivided superficial MB into complete and incomplete based on the full or partial encasement of the LAD within the left ventricular myocardium (20).

Average HR differences were calculated by subtracting the lower HR from the higher HR during the CT scan (29, 30).

Statistical Analysis

The SPSS software package (version 17.0; SPSS, Chicago, IL) was used for the statistical data analysis. Statistical significance was set at p values < 0.05. A one-way ANOVA (analysis of variance) test was performed to analyze the length of the three types of MB. In the descriptive statistical analysis, quantitative variables were expressed as means $\pm$ standard deviations, whereas categorical variables were expressed as frequencies or percentages.

RESULTS

Seventy-eight of the 1,353 DSCT examinations were excluded from the study analysis because of poor image quality, a cardiac motion artifact related to tachycardia and severe arrhythmia (n = 66) (mean HR 78.4 $\pm$ 13.2 bpm [41–132 bpm], an HR difference of 63.5 $\pm$ 28.7 bpm [range, 31–109 bpm]), or poor enhancement of the coronary artery (n = 12). Patients' characteristics is summarized in Table 1.

Among the remaining 1,275 patients, the image quality of the LAD was all diagnostic (excellent: 1,092, good: 178, fair: 5). The mean HR was 64.4 $\pm$ 7.6 bpm (range, 37–102 bpm), and the HR difference was 10 $\pm$ 14.9 bpm (range, 1–105 bpm) during DSCT. Of the 107 patients with an HR difference $\geq$ 30 bpm, 41 patients (38%) showed diagnostic image quality.

A total of 536 (226 males, 310 females; mean age, 58.6 $\pm$ 11.8 years; age range 24–90 years) out of 1,275 (42%) patients showed 557 cases of MB. Of the 557 tunneled

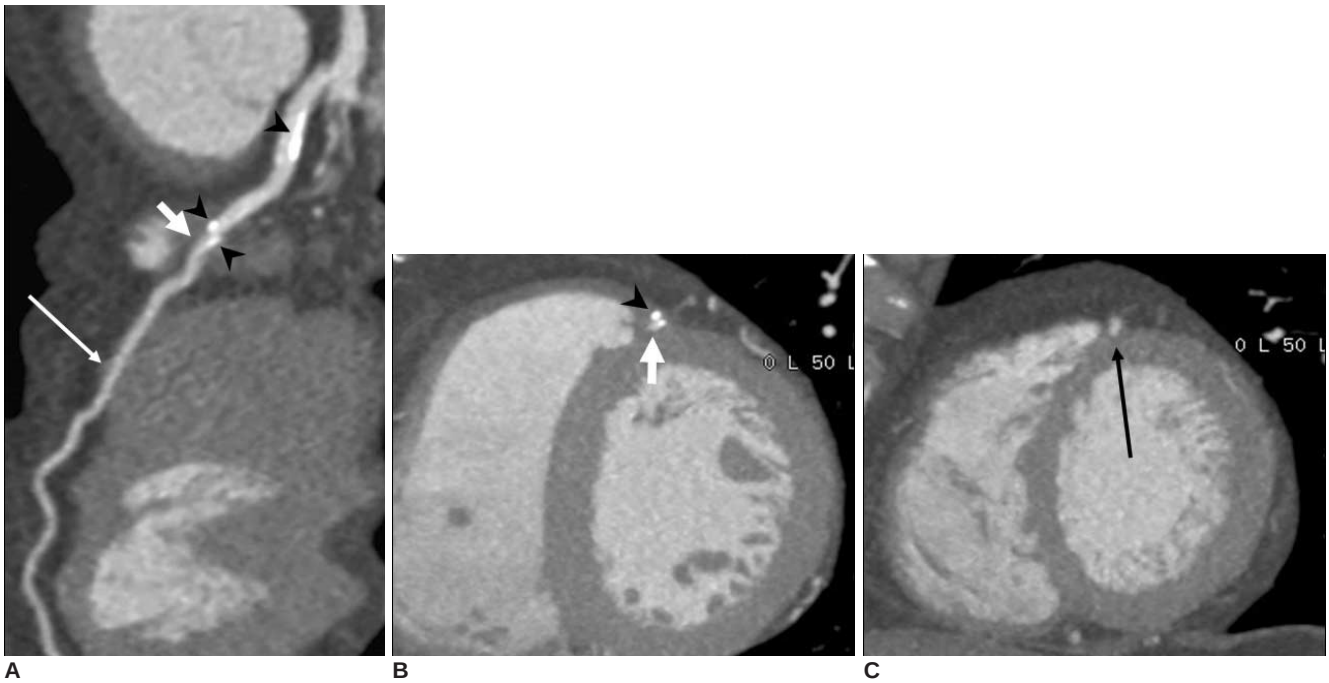

Fig. 3. 57-year-old man presented with angina.
Curved (**A**) and short-axis (**B, C**) multiplanar reformation images showed two tunneled segments (short and long arrows) in mid-left anterior descending coronary artery as well as calcified plaques (arrowheads) in segment proximal to myocardial bridging (**A**) and in tunneled segment (**A, B**).

segments, 529 (95%) were located in the mid LAD, 19 (3%) were located in the distal LAD, 2 (0.4%) were located in the proximal LAD, four (0.7%) were located in the proximal to mid LAD, and three (0.5%) were located in the mid to distal LAD. Nineteen patients had two areas of MB (Fig. 3), whereas one patient had three areas of MB in the LAD. The superficial MB type ($\leq$ 1 mm in depth) was seen in 368 of 557 (66%) of all of the tunneled LAD segments. Of the superficial forms of MB, the complete type was seen in 128 of 368 (35%) of cases, whereas the incomplete type was seen in 240 of 368 (65%) cases. The deep MB type (> 1 mm in depth) was seen in 189 of 557 (34%) tunneled LAD segments (Fig. 4). The mean length of a tunneled segment was 21.0 $\pm$ 11.6 mm. Superficial MB length as determined by CT was 16.4 $\pm$ 8.6 mm and deep MB length was 27.6 $\pm$ 12.8 mm. The mean length of the complete type (17.4 $\pm$ 8.3 mm) and incomplete type (16.0 $\pm$ 8.7 mm) were also determined. The mean lengths of the three types of MB were significantly different from one another ($p < 0.05$). The mean depth of a tunneled segment of deep MB as determined on CT was 3.0 $\pm$ 1.4 mm.

Atherosclerotic plaques were associated with MB in 175 (31%) of 557 tunneled segments (Fig. 3). Plaques were located 2 cm proximal to, within and distal to areas of MB in 87 (91%), 3 (2%) and 13 (7%) cases, respectively. Atherosclerotic plaques in a 2-cm-long segment proximal to the entry of the tunneled segment were found in 87 of 557 cases (16%); of the tunneled segments, 17 were the complete superficial type, 29 were the incomplete superficial type, and 41 were the deep type.

DISCUSSION

This study showed that the depiction rate of MB was 42% in a large, heterogeneous patient population. In addition to depicting the morphological features of MB, including the length and depth of tunneled the segments, DSCT-CA showed the precise location of MB and evaluated concomitant coronary atherosclerosis proximal to an area of MB.

The incidence of MB varies widely between the CCA series (0.5–16%) and autopsy series (15–85%). This discordance occurs because most patients with MB have unrelated overt symptoms that are rarely referred for CCA. In addition CCA is not sensitive enough to detect a 'milking effect' (temporary occlusion of the artery during systole) that is noted in the diagnosis of superficial MB (1–

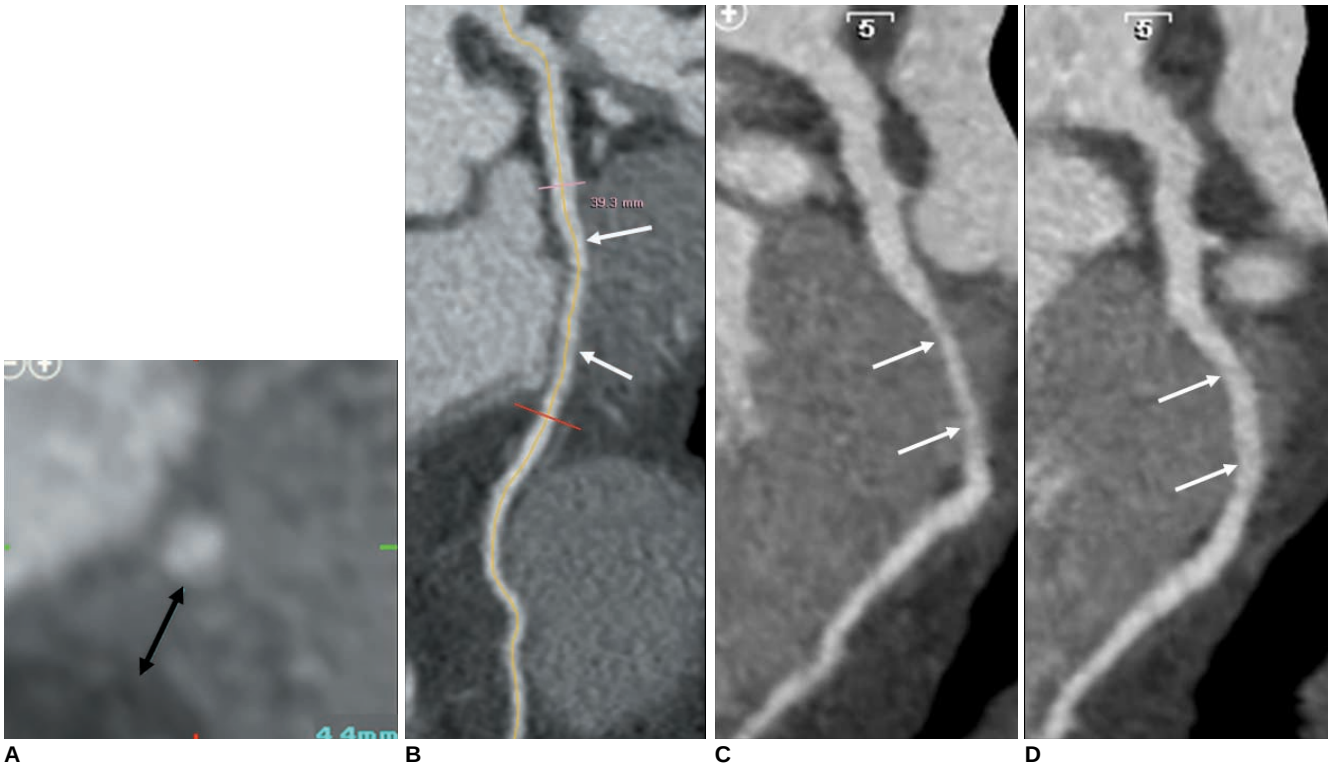

Fig. 4. 57-year-old man presented with atypical chest pain.
Depth (**A**) and length (**B**) of tunneled segment (arrows) of left anterior descending coronary artery were 4.4 mm and 39.3 mm, respectively. Systolic (**C**) and diastolic (**D**) curved multiplanar reformation images of tunneled left anterior descending coronary artery segment show that lumen of tunneled segment is compressed by myocardial contraction in systolic phase (**C**), but had normal diameter in diastolic phase (**D**). This phenomenon is known as 'milking effect'.

3). Also, an atherosclerotic plaque located at a segment proximal to a tunneled segment may hamper the detection of MB on CCA. According to recent studies, CTCA has been accepted as a reliable noninvasive imaging modality for the diagnosis of MB, because MDCT can provide information about the lumen and wall of the coronary arteries and the myocardium in any plane. MB can be depicted on CTCA even when there is no significant 'milking effect' as well as no change in vessel course on CCA (15, 19, 20).

Recent studies have suggested that the high temporal resolution of DSCT might allow for the visualization of significantly more segments that are of diagnostic image quality, owing to less motion artifact compared to the 64-section MDCT at lower HRs (31). Also, in comparison to single-source CTs, the high temporal resolution of DSCTs might provide images of full diagnostic image quality in patients with high HRs and even atrial fibrillation (32, 33). Meng et al. (34) reported that DSCT provides a high accuracy rate for the detection of significant CAD, even in patients with high HRs. Brodoefel et al. (35) reported that a plot of mean image quality against HR variability reveals a cutoff for good image quality at 29.9 beats per examination with DSCT. In our study, 41 out of 107 (38%) patients who had a difference in HR greater than 30 bpm, showed a relatively good diagnostic image quality. As a result, we assumed that the high temporal resolution of DSCT played a part in creating the relatively good image quality under difficult conditions.

Despite the exceptionally high detection rate (58% and 44%) of MB by MDCT reported by Kim et al. (20) and Lubarsky et al. (24), the usual depiction rate using MDCT ranges from 4% to 31% (10–18, 21–23, 25–27, 36–39). The previous study using DSCT by Lu et al. (19) showed that the depiction rate of MB was 30%, and the MB was diagnosed when at least half of the coronary artery was embedded within the myocardium. The relatively higher depiction rate of MB by DSCT in our study (42%) can be explained by the use of a DSCT scanner, which is a dedicated vessel analysis software used to delineate MB, as well as the inclusion of the incomplete type of superficial MB (19, 20).

MB can be classified as superficial or deep, depending on the thickness of the covering muscular layer ($\leq$ 1 mm or > 1 mm), even though there are no clear-cut in-depth criteria for the classification of MB depicted on CT (12). In addition, superficial MB can be classified as complete or incomplete in accordance with the extent of the vessel encasement by the myocardium. Because systolic compression can occur in coronary segments without overlying muscle (20), subdivision of superficial MB into complete and incomplete types is acceptable in our study. The prevalence of superficial MB (66%) was higher than that of deep MB (34%). Furthermore, about two-thirds of cases of superficial MB were considered to be incomplete MB.

It is well known that tunneled coronary segments rarely contain atherosclerotic plaques (21). We also observed that most atherosclerotic plaques were located at the segment proximal to the tunneled segment (91%). This result is higher than those of several studies (12, 22).

This study has some important limitations. First, there is no certain definition of deep and superficial MB. Our cut-off value is similar to that of Konen et al. (12). The definition of incomplete MB is based on the classification of vessel encasement by the myocardium (20). Second, the measurements of the depth and length of the tunneled segments were not performed separately by each investigator. Thus, intra- and inter-observer variability could not be obtained. Third, we focused on the detection of MB and the evaluation of morphological features on CT. Also, we used the ECG-dependent dose modulation technique in many cases (77%, 984/1,275) to reduce the radiation dose during CTCA. Therefore, the luminal diameter of the LAD before MB and the smallest diameter of the tunneled segment were not measured. Fourth, CCA data were only available in 30 of the 1,275 patients with MB detected with CT; thus, we could not compare the morphologic features of MB between CT and CCA. Fifth, the study did not investigate the relationship between MB and clinical symptoms. Dedicated clinical studies would be required to determine if MB is responsible for symptoms such as angina, myocardial infarction, and life-threatening arrhythmias. Finally, this was a single-institution study. A large multicenter study would be necessary to determine the real incidence of MB *in vivo*.

In conclusion, the depiction rate of MB of the LAD was 42% using DSCT-CA, which also showed that two-thirds of MB segments were of the superficial type. The high temporal resolution of DSCT is helpful to more accurately detect and characterize MB despite the HR variability.

References

1. Möhlenkamp S, Hort W, Ge J, Erbel R. Update on myocardial bridging. *Circulation* 2002;106:2616-2622
2. Alegria JR, Herrmann J, Holmes DR Jr, Lerman A, Rihal CS. Myocardial bridging. *Eur Heart J* 2005;26:1159-1168
3. Kramer JR, Kitazume H, Proudfit WL, Sones FM Jr. Clinical significance of isolated coronary bridges: benign and frequent condition involving the left anterior descending artery. *Am Heart J* 1982;103:283-288
4. Noble J, Bourassa MG, Petitclerc R, Dyrda I. Myocardial bridging and milking effect of the left anterior descending coronary artery: normal variant or obstruction? *Am J Cardiol* 1976;37:993-999

5. Rossi L, Dander B, Nidasio GP, Arbustini E, Paris B, Vassanelli C, et al. Myocardial bridges and ischemic heart disease. *Eur Heart J* 1980;1:239-245
6. Bourassa MG, Butnaru A, Lespérance J, Tardif JC. Symptomatic myocardial bridges: overview of ischemic mechanisms and current diagnostic and treatment strategies. *J Am Coll Cardiol* 2003;41:351-359
7. Amoroso G, Battolla L, Gemignani C, Panconi M, Petronio AS, Rondine P, et al. Myocardial bridging on left anterior descending coronary artery evaluated by multidetector computed tomography. *Int J Cardiol* 2004;95:335-337
8. Goitein O, Lacomis JM. Myocardial bridging: noninvasive diagnosis with multidetector CT. *J Comput Assist Tomogr* 2005;29:238-240
9. Ko SM, Kim KS. Multidetector-row CT coronary angiographic finding of myocardial bridging. *Br J Radiol* 2007;80:E196-E200
10. Kantarci M, Duran C, Durur I, Alper F, Onbas O, Gulbaran M, et al. Detection of myocardial bridging with ECG-gated MDCT and multiplanar reconstruction. *AJR Am J Roentgenol* 2006;186:S391-S394
11. Zeina AR, Odeh M, Blinder J, Rosenschein U, Barmeir E. Myocardial bridge: evaluation on MDCT. *AJR Am J Roentgenol* 2007;188:1069-1073
12. Konen E, Goitein O, Sternik L, Eshet Y, Shemesh J, Di Segni E. The prevalence and anatomical patterns of intramuscular coronary arteries: a coronary computed tomography angiographic study. *J Am Coll Cardiol* 2007;49:587-593
13. Kawawa Y, Ishikawa Y, Gomi T, Nagamoto M, Terada H, Ishii T, et al. Detection of myocardial bridge and evaluation of its anatomical properties by coronary multislice spiral computed tomography. *Eur J Radiol* 2007;61:130-138
14. Ko SM, Choi JS, Nam CW, Hur SH. Incidence and clinical significance of myocardial bridging with ECG-gated 16-row MDCT coronary angiography. *Int J Cardiovasc Imaging* 2008;24:445-452
15. Leschka S, Koepfli P, Husmann L, Plass A, Vachenauer R, Gaemperli O, et al. Myocardial bridging: depiction rate and morphology at CT coronary angiography--comparison with conventional coronary angiography. *Radiology* 2008;246:754-762
16. Hazirolan T, Canyigit M, Karcaaltincaba M, Dagoglu MG, Akata D, Aytemir K, et al. Myocardial bridging on MDCT. *AJR Am J Roentgenol* 2007;188:1074-1080
17. Konen E, Goitein O, Di Segni E. Myocardial bridging, a common anatomical variant rather than a congenital anomaly. *Semin Ultrasound CT MRI* 2008;29:195-203
18. Jodocy D, Aglan I, Friedrich G, Mallouhi A, Pachinger O, Jaschke W, et al. Left anterior descending coronary artery myocardial bridging by multislice computed tomography: correlation with clinical findings. *Eur J Radiol* 2010;73:89-95
19. Lu GM, Zhang LJ, Guo H, Huang W, Merges RD. Comparison of myocardial bridging by dual-source CT with conventional coronary angiography. *Circ J* 2008;72:1079-1085
20. Kim PJ, Hur G, Kim SY, Namgung J, Hong SW, Kim YH, et al. Frequency of myocardial bridges and dynamic compression of epicardial coronary arteries: a comparison between computed tomography and invasive coronary angiography. *Circulation* 2009;119:1408-1416
21. Canyigit M, Hazirolan T, Karcaaltincaba M, Dagoglu MG, Akata D, Aytemir K, et al. Myocardial bridging as evaluated by 16 row MDCT. *Eur J Radiol* 2009;69:156-164
22. Jacobs JE, Bod J, Kim DC, Hecht EM, Srichai MB. Myocardial bridging: evaluation using single- and dual-source multidetector cardiac computed tomographic angiography. *J Comput Assist Tomogr* 2008;32:242-246
23. La Grutta L, Runza G, Lo Re G, Galia M, Alaimo V, Grassedonio E, et al. Prevalence of myocardial bridging and correlation with coronary atherosclerosis studied with 64-slice CT coronary angiography. *Radiol Med* 2009;114:1024-1036
24. Lubarsky L, Gupta MP, Hecht HS. Evaluation of myocardial bridging of the left anterior descending coronary artery by 64-slice multidetector computed tomographic angiography. *Am J Cardiol* 2007;100:1081-1082
25. Zhang LJ, Yang GF, Zhou CS, Huang W, Lu GM, Shiroishi MS. Multiphase evaluation of myocardial bridging with dual-source computed tomography. *Acta Radiol* 2009;50:775-780
26. Johansen C, Kirsch J, Araoz P, Williamson E. Detection of myocardial bridging by 64-row computed tomography angiography of the coronaries. *J Comput Assist Tomogr* 2008;32:448-451
27. Chen YD, Wu MH, Sheu MH, Chang CY. Myocardial bridging in Taiwan: depiction by multidetector computed tomography coronary angiography. *J Formos Med Assoc* 2009;108:469-474
28. Matt D, Scheffel H, Leschka S, Flohr TG, Marincek B, Kaufmann PA, et al. Dual-source CT coronary angiography: image quality, mean heart rate, and heart rate variability. *AJR Am J Roentgenol* 2007;189:567-573
29. Blankstein R, Shturman LD, Rogers IS, Rocha-Filho JA, Okada DR, Sarwar A, et al. Adenosine-induced stress myocardial perfusion imaging using dual-source cardiac computed tomography. *J Am Coll Cardiol* 2009;54:1072-1084
30. Ko SM, Kim NR, Kim DH, Song MG, Kim JH. Assessment of image quality and radiation dose in prospective ECG-triggered coronary CT angiography compared with retrospective ECG-gated coronary CT angiography. *Int J Cardiovasc Imaging* 2010;26:93-101
31. Baumüller S, Leschka S, Desbiolles L, Stolzmann P, Scheffel H, Seifert B, et al. Dual-source versus 64-section CT coronary angiography at lower heart rates: comparison of accuracy and radiation dose. *Radiology* 2009;253:56-64
32. Donnino R, Jacobs JE, Doshi JV, Hecht EM, Kim DC, Babb JS, et al. Dual-source versus single-source cardiac CT angiography: comparison of diagnostic image quality. *AJR Am J Roentgenol* 2009;192:1051-1056
33. Wang Y, Zhang Z, Kong L, Song L, Merges RD, Chen J, et al. Dual-source CT coronary angiography in patients with atrial fibrillation: comparison with single-source CT. *Eur J Radiol* 2008;68:434-441
34. Meng L, Cui L, Cheng Y, Wu X, Tang Y, Wang Y, et al. Effect of heart rate and coronary calcification on the diagnostic accuracy of the dual-source CT coronary angiography in patients with suspected coronary artery disease. *Korean J Radiol* 2009;10:347-354
35. Brodoefel H, Burgstahler C, Tsiflikas I, Reimann A, Schroeder S, Claussen CD, et al. Dual-source CT: effect of heart rate, heart rate variability, and calcification on image quality and diagnostic accuracy. *Radiology* 2008;247:346-355
36. Bayrak F, Degertekin M, Eroglu E, Guneysu T, Sevinc D, Gemici G, et al. Evaluation of myocardial bridges with 64-slice computed tomography coronary angiography. *Acta Cardiol* 2009;64:341-346
37. Jeong YH, Kang MK, Park SR, Kang YR, Choi HC, Hwang SJ,

et al. A head-to-head comparison between 64-slice multidetector computed tomographic and conventional coronary angiographies in measurement of myocardial bridge. *Int J Cardiol* 2009 [Epub ahead of print]
38. Kim SY, Lee YS, Lee JB, Ryu JK, Choi JY, Chang SG, et al. Evaluation of myocardial bridge with multidetector computed tomography. *Circ J* 2010;74:137-141
39. Atar E, Kornowski R, Fuchs S, Naftali N, Belenky A, Bachar GN. Prevalence of myocardial bridging detected with 64-slice multidetector coronary computed tomography angiography in asymptomatic adults. *J Cardiovasc Comput Tomogr* 2007;1:78-83